Hindawi
Journal of Chemistry
Volume 2017, Article ID 3621084, 7 pages
https://doi.org/10.1155/2017/3621084

Research Article

Application of Spent Li-Ion Batteries Cathode in Methylene Blue Dye Discoloration

Eric M. Garcia, Hosane A. Taroco, Ana Paula C. Madeira, Amauri G. Souza, Rafael R. A. Silva, Júlio O. F. Melo, Cristiane G. Taroco, and Quele C. P. Teixeira

DECEB, Federal University of São João del-Rei, Campus Sete Lagoas, MG-424, Km 45, 35701-970 Sete Lagoas, MG, Brazil

Correspondence should be addressed to Eric M. Garcia; ericmgmg@hotmail.com

Received 22 December 2016; Revised 4 March 2017; Accepted 26 March 2017; Published 30 May 2017

Academic Editor: Carlos Alberto Lberto Martínez-Huitle

This paper aims to present the mechanism study of methylene blue (MB) discoloration using spent Li-ion battery cathode tape and hydrogen peroxide. The recycled cathode used in this work is composed of 72% of $LiCoO_2$, 18% of carbon, and 10% of Al. The value found for surface area is 8.9 m^2/g and the ZCP value occurs in pH = 2.95. Different from what is proposed in the literature, the most likely mechanism of methylene blue discoloration is the oxidation/delitiation of $LiCoO_2$ and the reduction of H_2O_2 forming $OH^{\bullet}$. Thus, in this paper, an important and promising alternative for discoloration of textile industry dyes using spent Li-ion battery cathode is presented.

1. Introduction

1.1. Li-Ion Battery Recycling: A Brief Overview. The fast popularization of portable devices such as cell phones is due mostly to the introduction of Li-ion batteries (LIBs) by Sony in 1991 [1–3]. The introduction of LIBs to the market was due to characteristics such as high energy density, long lifespan, and lightweight [3, 4]. In general, LIBs have no Cd, unlike Ni-Cd batteries, and have much less Ni than Ni-MH batteries. The cathode material widely used in LIBs is lithium and cobalt oxide, $LiCoO_2$ [1–3, 5]. Due to their widespread use, LIBs' disposal is a topic of great relevance. The waste generated by LIBs will soon be a dramatic problem in countries such as China, where the quantity of discarded LIBs in 2020 can reach 25 billion units [6]. Among many applications, it is reported that the spent $LiCoO_2$ catalyzes methylene blue degradation in the presence of H_2O_2 [3]. Thus, a very audacious project concerns the application of recycled materials from LIBs on waters contaminated with potentially toxic organic molecules. This process is very interesting concerning the environment due to the possibility of promoting the decontamination of organic pollutants using a residue coming from Li-ion battery waste. The substances traditionally used for organic decontamination are O_3 and H_2O_2 [7]. However, the cost of these compounds is relatively high (O_3 is \$2.2 per kg and H_2O_2 is \$1.5 per kg) [7]. The use of $LiCoO_2$ increases the velocity constant of methylene blue (MB) degradation 200 times if compared to pure H_2O_2 with minimum additional cost since this material comes from spent LIB [3]. Thus, the use of recycled LIB cathode is an excellent alternative for degradation of potentially toxic organic molecules. The literature reports hydrogen peroxide oxidation, promoted by $LiCoO_2$ reduction, with intermediate step correspondent to $O_2^{-\bullet}$ radical formation [3]. However, we have reasons to believe that the methylene blue discoloration mechanism, using the H_2O_2 and LIB spent cathode, is different from what is proposed in the literature [3]. The main controversial point is that the reduction potential of $LiCoO_2$ in aqueous solution (see (1)) is around −0.95 V [4] and oxidation of H_2O_2 (see (2)) is −0.89 V [3]. Thus, the global process (see (3)) is thermodynamically unfavorable (−1.84 V). Thus, the pathway to understand the reaction mechanism between $LiCoO_2$ and H_2O_2 involves predominantly the study of the chemical behavior of $LiCoO_2$ in aqueous solution.

$$4H_2O + 2LiCoO_{2(s)} + 2e^- \longrightarrow 4OH^-_{(aq)} + 2Co(OH)_{2(s)} + 2Li^+_{(aq)} \quad (1)$$

$$E^o = -0.95\ \text{V}$$

$$2H_2O_{2(aq)} \longrightarrow 4H^+ + 2e^- + 2O_{2(g)}^{-\bullet} \quad E^o = -0.89\,V \tag{2}$$

$$2LiCoO_{2(s)} + 2H_2O_2 \longrightarrow 2Co(OH)_{2(s)} + 2Li^+_{(aq)} + 2O_{2(g)}^{-\bullet} \quad E^o = -1.84\,V \tag{3}$$

1.2. The Chemical Behavior of $LiCoO_2$ in Aqueous Solution. The LIB operating system basically consists of reversible extraction/insertion of Li^+ ions between two electrodes (see (4)) [1, 8, 9]. For LIB with $LiCoO_2$ cathode, in the charge process, the Li^+ intercalated in the $LiCoO_2$ structure is forced out by an external applied potential in direction of a carbonaceous matrix (see (4)) [1]. In the discharge (reverse process), the Li^+ ions return to the $Li_{(1-x)}CoO_2$ matrix due to a concentration gradient [1]. Due to the large LIB operation potential, the electrolyte is a nonaqueous solution composed of lithium salts, such as 1 M $LiPF_6$, in alkyl organic carbonates (ethylene, propylene, and dimethyl carbonates) [9].

$$C_{6(s)} + LiCoO_{2(s)} \underset{\text{discharge}}{\overset{\text{charge}}{\rightleftharpoons}} Li_xC_{6(s)} + Li_{(1-x)}CoO_{2(s)} \quad E \cong 3.7\,V \tag{4}$$

In fact, in aqueous electrolyte with electrode materials $LiCoO_2$ and C_6, the reversible intercalation/deintercalation of Li^+ happens under potential equal to 1.20 V (99% of Coulomb efficiency) [10]. The $LiCoO_2$ charge in aqueous solution (delitiation) begins around 1.02 V [10] practically independent of the pH value [11].

$$LiCoO_{2(s)} \longrightarrow Li_{(1-x)}CoO_{2(s)} + xLi^+_{(sol)} + xe^- \tag{5}$$

Thus, to force the deintercalation of Li^+ ions from $LiCoO_2$ lamellar structure without an external power source, it is necessary to use an oxidant agent with reduction potential higher than 1.02 V. The reduction potential of H_2O_2/H_2O [12] and O_2/H_2O [12] (considering $P_{O2} = 0.21$ atm) versus pH is shown in Figure 1. The dotted line represents the limit potential (1.02 V) for $LiCoO_2$ oxidation in aqueous solution (see (5)). The redox reaction represented by $LiCoO_2$ oxidation and the reduction of H_2O_2 (see (6)) are spontaneous along the pH range 1 to 12. The potential for (6) considering pH =7 is 0.3 V (details in Figure 1). The interference of parallel O_2 reduction is observed only in pH <1 (Figure 1).

$$2xH^+_{(aq)} + xH_2O_{2(aq)} + 2LiCoO_{2(s)} \longrightarrow 2Li_{(1-x)}CoO_{2(s)} + 2xLi^+_{(aq)} \tag{6}$$

On the other hand, for acid pH values, the cointercalation of H^+ ions in the charged $Li_{(1-x)}CoO_2$ (see (7)) [13] normally promotes the obstruction of Li^+ diffusion pathways [11].

$$1e^- + H^+ + Li_{(1-x)}CoO_2 \longrightarrow Li_{(1-x)}HCoO_2 \tag{7}$$

Thus, this paper aims to present the mechanism study of methylene blue (MB) discoloration using LIB spent cathode tape and hydrogen peroxide. The spent cathode tape was characterized by X-ray diffraction, atomic absorption spectrophotometry (AAS), zeta potential, SEM, and the MB adsorption technique to determine the surface area.

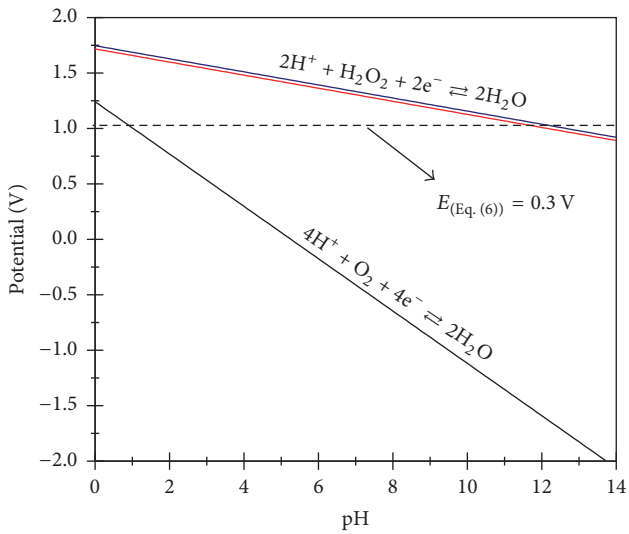

Figure 1: Potential versus pH for O_2 and H_2O_2 reduction in water [Haynes]. The dotted line (1.02 V) represents the limit potential for $LiCoO_2$ oxidation (delitiation) in water. It was considered that $P_{O2} = 0.21$ atm, $[H_2O_2] = 0.10\,mol\,L^{-1}$ (blue line), and $[H_2O_2] = 0.01\,mol\,L^{-1}$ (red line).

Figure 2: Cathode, anode, and separator from a cell phone spent LIB used in this work.

2. Materials and Methods

2.1. The Characterizations of LIB Spent Cathode. The LIB used in this paper was a spent cell phone battery. The LIB was dismantled using the manual procedure and the components were separated (Figure 2). The spent cathode in tape form was

Table 1: The experimental conditions used in the reaction order study of MB discoloration. The variables were spent cathode (SC) area and H_2O_2 and MB concentration.

	Condition 1	Condition 2	Condition 3	Condition 4
	SC = 16 cm^2	SC = 16 cm^2	SC = 4 cm^2	SC = 16 cm^2
	$[H_2O_2]$ = 0.1 M	$[H_2O_2]$ = 0.01 M	$[H_2O_2]$ = 0.1 M	$[H_2O_2]$ = 0.1 M;
	MB = 12 ppm	MB = 12 ppm	MB = 12 ppm	MB = 6 ppm
t_{50}	60 s	67 s	242 s	32 s

separated and, to remove the organic solvents, it was heated at 200°C for 5 h according to the literature [1].

2.1.1. The Crystalline Structure. The spent cathode tape was characterized by X-ray diffraction on a 200 B Rotaflex-Rigaku with Cu Kα irradiation, a Cu filter, and scanning speed of 2° min^{-1}. The spent cathode after degradation of MB was also characterized to verify the possible presence of Co_3O_4 phase.

2.1.2. Atomic Absorption Spectrophotometry (AAS). The spent cathode powder was scraped from the current collector. 0.20 g of the cathode powder was dissolved in 250 mL of 2 M H_2SO_4 (Sigma-Aldrich, purity ≥ 98%) and 6 mL of 35% w/w H_2O_2 (Sigma-Aldrich). The resulting solution was filtered and analyzed by AAS on a Hitachi Z8200.

2.1.3. Zeta Potential. The zeta potential was determined by Dynamic Light Scattering (DLS) measurements on a Zeta-Sizer Malvern at 25°C in an aqueous medium after dispersion for 30 min in an ultrasound bath.

2.1.4. Scanning Electron Microscopy (SEM). The morphology of the spent Li-BCT was observed by Field-Emission Scanning Electron Microscopy on a JEOL JXA model 8900 RL.

2.1.5. Determination of Surface Area. A successful method to determine the active area was described in the *literature* in recent years. It is based on the adsorption of MB [14]. The measure of the surface area with MB adsorption has the main advantage of measuring the surface accessible to electrolyte. To determine the surface area, the LIB spent cathode was cut into rectangular pieces of 4 cm^2 (~60 mg) and put into a MB (Sigma-Aldrich, dye content ≥95%) solution with different concentrations (1, 2, 3, 5, 7, and 10 ppm) in different pH values (between 3 and 11). After 24 h, the MB concentration was monitored using a UV-spectrophotometer FEMTO Cirrus 80 PR at 659 nm. The MB dye adsorption capacity (q_e) was determined by (8) [15], in which C and C_e are the initial and equilibrium MB concentration, respectively. For the determination of the surface area, the Langmuir isotherm (see (9)) was considered, in which q_{max} is the monolayer adsorption capacity (mg/g) and K_L is a constant related to free energy of adsorption [15]. To convert q_{max} into surface area (m^2/g), each MB molecule with $1{,}70 \times 10^{-18}$ m^2 [14] was considered.

$$q_e = \frac{V(C - C_e)}{m}, \tag{8}$$

$$\frac{C_e}{q_e} = C_e\left(\frac{1}{q_{max}}\right) + \frac{1}{q_{max}K_L}. \tag{9}$$

2.2. Methylene Blue Discoloration Mechanism. To study the kinetics of MB discoloration, a 100 mL glass cell containing 50 mL of MB solution, H_2O_2, and LIB spent cathode tape (cut into rectangular pieces) was stirred magnetically (10 rpm) in a bath with controlled temperature at 25°C. Before the H_2O_2 addition, the MB solution was put in contact with LIB spent cathode tape for 24 hours to establish the adsorption equilibrium. The pH of the solution was adjusted at around 7 (exactly 7.02). The discoloration process was monitored by analyzing aliquots at 659 nm. The reaction order was evaluated by variation of spent cathode area and H_2O_2 and MB concentration. The variations of the parameters are shown in Table 1. Considering t_{50} as the interval of time to promote 50% of discoloration, the reaction order (a_R) in relation to generic reactant "R" can be obtained by (10) [3] in which t_{50} and t'_{50} are the interval of time to promote 50% of discoloration in two different concentrations represented by $[R]$ and $[R]'$, respectively.

$$a_R = \frac{\log\left(t'_{50}/t_{50}\right)}{\log\left([R]/[R]'\right)}. \tag{10}$$

The active radical was identified by the addition of 2 M isopropanol (i-PrOH) as a scavenger for $OH^{\bullet}$ [16]. The cyclic experiment was performed using the same spent cathode in 5 cycles of MB discoloration (600 min). All measurements were made in the absence of visible light to avoid the possible electron excitation of cobalt lithium oxide conduction band to the valence band generating the electron (BC) and hole (BV) pair. After MB discoloration, the resultant solution was analyzed with AAS aiming to determine the possible lixiviation of Co and Li.

3. Results and Discussion

3.1. The Characterizations of LIB Spent Cathode Powder. The characterization of LIB spent cathode is very important since its composition can present Fe, Mn, and Ni. Thus, X-ray

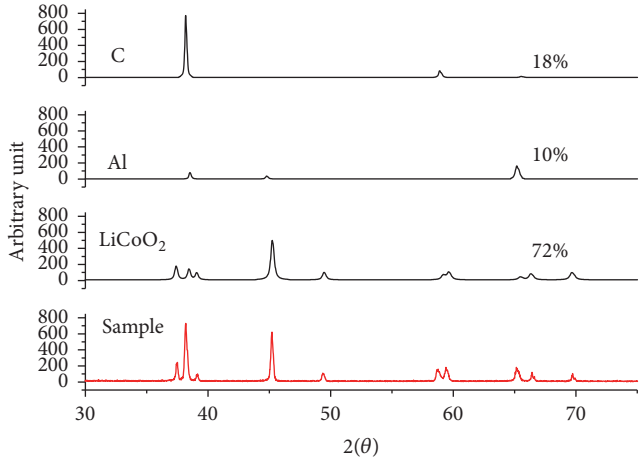

Figure 3: The X-ray diffractogram of LIB spent cathode tape before MB discoloration reaction. The proportion of phase was analyzed with Rietveld method using the free software FullProf©.

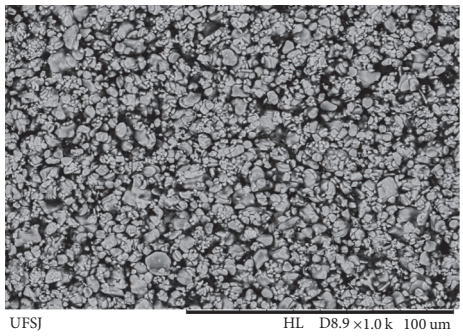

Figure 4: Scanning Electron Microscopy (SEM) of LIB spent cathode tape.

diffraction and AAS were used to elucidate the chemical composition of LIB spent cathode. The spent cathode powder was dissolved (Materials and Methods) and the resulting solution was analyzed by AAS. The presence of Fe, Mn, and Ni was not detected (detection limit: 0.04 ppm). The Li and Co concentrations were 55 ppm and 418 ppm, respectively. Considering the atomic mass of Co and Li (58.933 and 6.941 g/mol [12]), these concentrations are compatible with a stoichiometric proportion of approximately 1 : 1. The X-ray of LIB spent cathode tape was analyzed with Rietveld method using the free software FullProf© [17] (Figure 3). The X-ray diffraction showed the proportion of phases present in the cathode. The recycled cathode is composed of 72% of $LiCoO_2$, 18% of carbon, and 10% of Al. Carbon is added to increase the electrical conductivity of the cathodic material [1]. The Al presence is due to the current collector composition and its detection in X-ray diffraction is possible due to the porosity of the LIB cathode [1]. It is worth pointing out that the presence of other Li_xCoO_2 phases (with x varying from 1 to 0.5) is also possible, but their detection through X-ray diffraction is complex when $0.5 < x < 1$ [11].

Figure 4 shows the Scanning Electron Microscopy (SEM) of the spent cathode from Li-ion battery. The values found

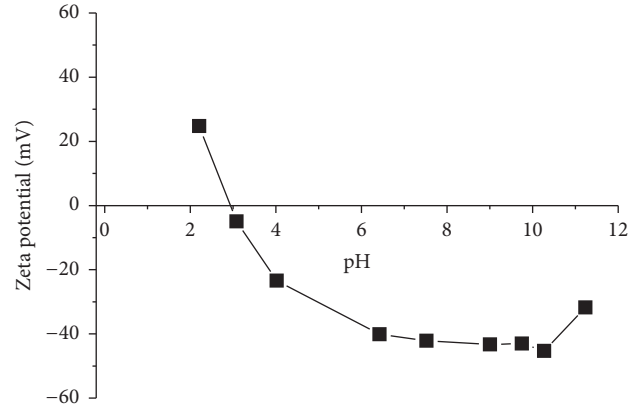

Figure 5: Zeta potential of LIB spent cathode powder.

for the porosity and the average size of grain were 42% and 31 μm, respectively [18].

To clarify the adsorption process, the zeta potential was assessed (Figure 5). The zeta potential remains practically constant (~−40 mV) in the pH ranging from 11 to 6. Considering the values of pH ranging from 6 to 3, the zeta potential varies considerably until it reaches the zero charge point (ZCP). The spent cathode has relatively acidic ZCP (close to pH = 2.95).

To determine the surface area, Figure 6(a) shows the C_e/q_e versus C_e plot for MB adsorption onto the spent LIB cathode. The adjustment of experimental points in Langmuir isotherm (see (9)) showed good concordance ($R^2 = 0.99$). Similar to the zeta potential measurement, the surface area measured by MB adsorption undergoes a variation with pH (Figure 6(b)). For values of pH ranging from 11 to 6, the surface area changes minimally. The value found for surface area based on MB adsorption was 8.9 m^2/g in pH = 7. With the pH ranging from 6 to 3, the MB adsorption decreases quite probably due to the H^+ adsorption competition.

3.2. Methylene Blue Discoloration Mechanism. To obtain the reaction order and the reaction determinant step (RDS), MB discoloration was performed in different conditions as shown in Figure 7. Table 1 shows t_{50} in different situations. The reaction orders obtained in relation to H_2O_2, SC (spent cathode), and MB are, respectively, $a_{H_2O_2} = 0.04 \approx 0$, $a_{SC} = 1{,}008 \approx 1$, and $a_{MB} = 1.102 \approx 1$. Thus, the reaction determinant step can be written as $\nu_{rds} = k[SC][MB]$.

To prove that the reaction mechanism can be represented by (6), the pH and Co and Li concentration were measured before and after the discoloration reaction. The experimental design is given by Table 1 in condition 3. In the previous solution, the concentrations of Co and Li were below the detection limit (0.04 ppm). After MB discoloration, the Co concentration remained below 0.04 ppm and the Li concentration reached 1.2 ppm. Moreover, after the discoloration reaction, the pH value ranged from 7.01 to 7.25. It is important to note that, for charged $Li_{(1-x)}CoO_2$ phase in aqueous solution, the Li^+ intercalation (which corresponds to the LIB discharge process) only must be considered favorable in

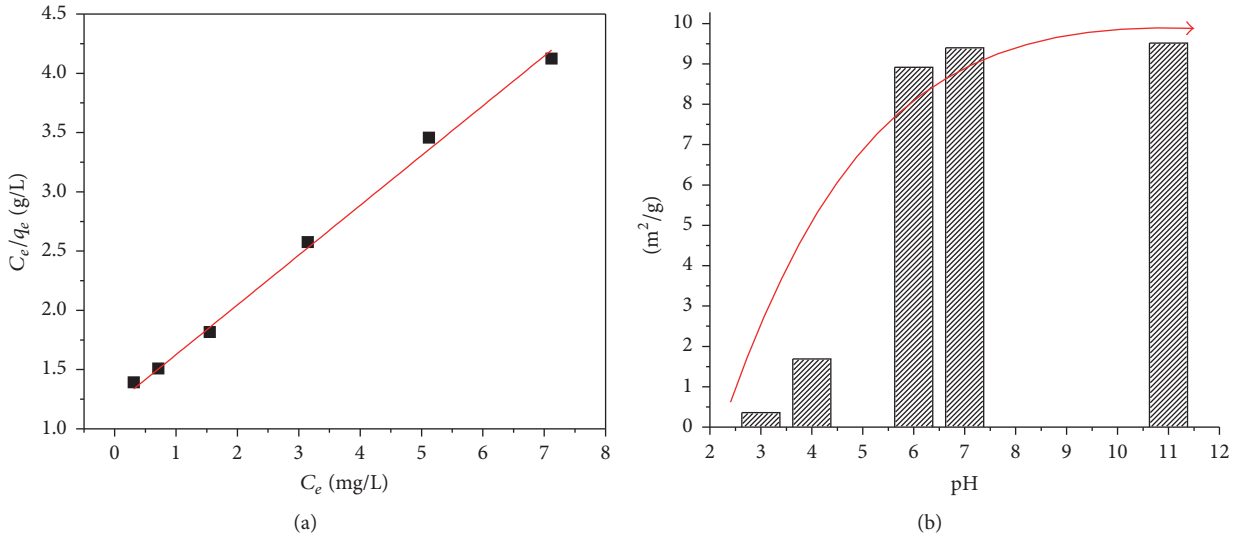

FIGURE 6: (a) The C_e/q_e versus C_e plot for MB adsorption onto spent LIB cathode. (b) The surface area measured by MB adsorption with pH variation.

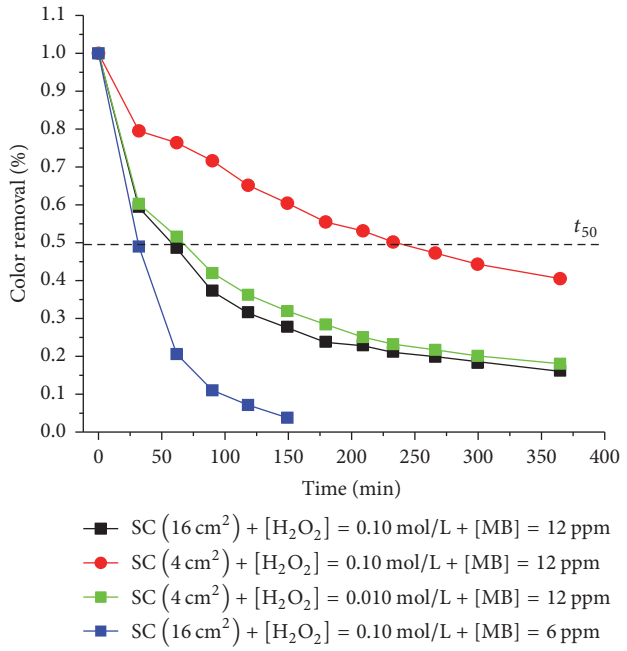

FIGURE 7: Process of MB discoloration (color removal) versus time for pH = 7.02 with different conditions of H_2O_2, spent cathode (SC), and MB solution.

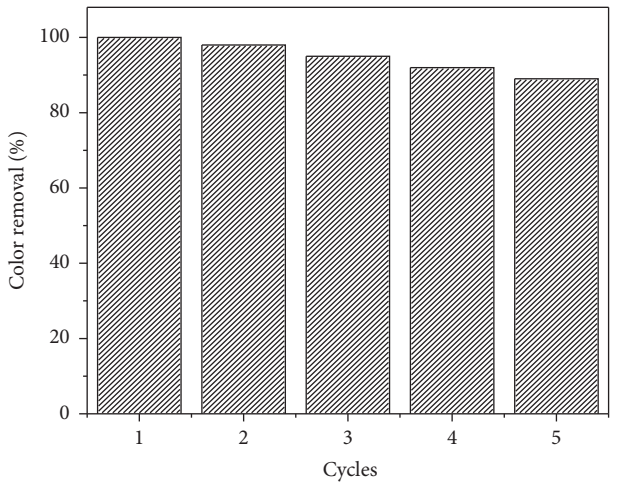

FIGURE 8: The result of five cyclic tests of MB discoloration. The experimental conditions used were MB 12 ppm, spent cathode 4 cm^2, and 0.1 M H_2O_2.

special conditions as reported in the literature (e.g., in 5 M $LiNO_3$) [10]. Thus, the only spontaneous process for $LiCoO_2$ under the experimental conditions used in this work is the oxidation process shown by (6). With the decrease of Li content in the cathode ($LiCoO_2$), there is also a decrease in the kinetics of MB discoloration. This is easily seen in the cyclic test performed with the same LIB spent cathode tape (Figure 8). A slight drop of discoloration capacity is noticed, which can be evidence that the spent cathode is a reagent and not a catalyst as reported previously in the literature [3]. Thus, the charged phase $Li_{(1-x)}CoO_2$ reacts in the oxidation direction by

$$\begin{aligned} Li_{(1-x)}CoO_{2(s)} \longrightarrow\ & (1-x-y)\,Li^{+}_{(aq)} \\ & + Li_{(1-x-y)}CoO_{2(s)} \\ & + (1-x-y)\,e^{-} \\ & \text{with} \longrightarrow 1 \geq x + y \end{aligned} \tag{11}$$

The X-ray diffraction was performed on the spent cathode after degradation of methylene blue. The main objective was to verify the presence of Co_3O_4. The charged Li_xCoO_2 (with $1 > x$) is metastable and, after the charge/discharge cycles,

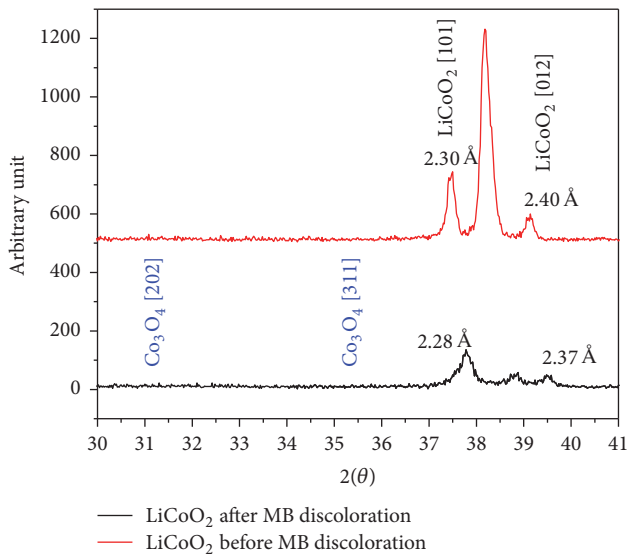

Figure 9: The X-ray diffractogram of LIB spent cathode tape before and after MB discoloration reaction (condition 3 in Table 1).

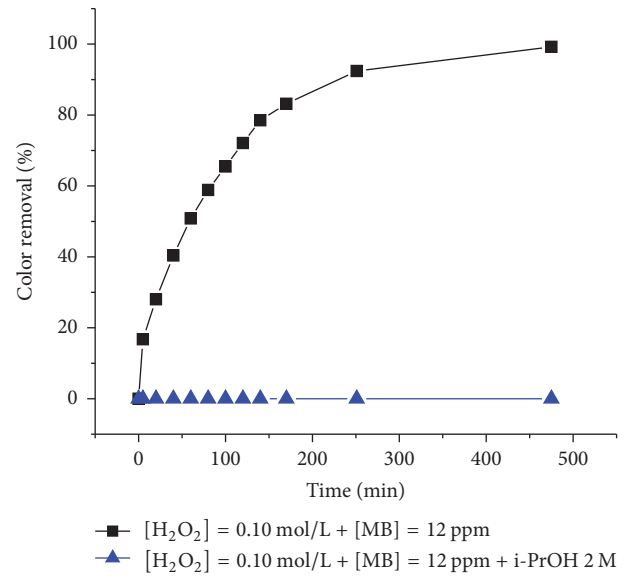

Figure 10: The discoloration of 12 ppm MB with 0.10 M H_2O_2 and spent cathode with and without 2 M i-PrOH.

the Co_3O_4 phase can be formed through the decomposition solid-state reaction (see (12)) [19].

$$Li_{0.5}CoO_2 \longrightarrow 0.5LiCoO_2 + 1/6Co_3O_4 + 1/6O_2 \quad (12)$$

This reaction takes place at around 190°C [19]. In this work, the most probable process involving $LiCoO_2$ is delitiation (LIB charge); in addition, the temperature of the reaction system did not exceed 25°C. Thus, after the methylene blue discoloration reaction, Co_3O_4 presence is not expected. Figure 9 shows the positions of the main peaks of Co_3O_4 phase (JCPDS 78-1970 [13]). In Figure 9, we observe only the presence of $LiCoO_2$ crystallographic planes. Thus, the presence of Co_3O_4 phase in the spent cathode after degradation of methylene blue is not confirmed by X-ray diffraction. It is noted that, in the spent cathode after MB discoloration reaction, the interplanar distance undergoes a subtle decrease, showing that the H^+ cointercalation also is not evidenced [11].

To confirm the mechanism, the active radicals were identified by the addition of isopropanol (i-PrOH) as a scavenger for $OH^\bullet$ [16]. Figure 10 shows the discoloration of 12 ppm MB with 0.1 M H_2O_2 and spent cathode with and without 2 M i-PrOH. The measure shows that $OH^\bullet$ is the predominant radical formed by H_2O_2 reduction (see (13)) promoted by $LiCoO_2$ oxidation.

$$H_2O_{2(aq)} + 1e^- \rightarrow OH^{-\bullet}_{(aq)} + OH^-_{(aq)} \quad (13)$$

4. Conclusion

In this paper, we presented an important and promissory alternative for discoloration of textile industry using LIB recycled cathode. The model molecule used was methylene blue. The recycled cathode is composed of 72% of $LiCoO_2$, 18% of carbon, and 10% of Al. The value found for surface area of the spent cathode was 8.9 m^2/g and the ZCP value occurs in pH = 2.95. Different from what is proposed in the literature, the more probable mechanism of methylene blue discoloration is the oxidation/delitiation of $LiCoO_2$ and the reduction of H_2O_2 forming the $OH^\bullet$.

Conflicts of Interest

The authors declare that they have no conflicts of interest regarding the publication of this paper.

Acknowledgments

This work was supported by CNPq, DECEB, Federal University of São João del-Rei (UFSJ), Sete Lagoas. This work is a collaboration research project of members of the Rede Mineira de Química (RQ-MG) supported by FAPEMIG (Project CEX-RED-00010-14).

References

[1] M. B. J. G. Freitas and E. M. Garcia, "Electrochemical recycling of cobalt from cathodes of spent lithium-ion batteries," *Journal of Power Sources*, vol. 171, no. 2, pp. 953–959, 2007.

[2] E. M. Garcia, V. D. F. C. Lins, H. A. Tarôco, T. Matencio, R. Z. Domingues, and J. A. F. Dos Santos, "The anode environmentally friendly for water electrolysis based in LiCoO2 recycled from spent lithium-ion batteries," *International Journal of Hydrogen Energy*, vol. 37, no. 22, pp. 16795–16799, 2012.

[3] M. C. Abreu Gonçalves, E. M. Garcia, H. A. Taroco et al., "Chemical recycling of cell phone Li-ion batteries: Application in environmental remediation," *Waste Management*, vol. 40, pp. 144–150, 2015.

[4] Y. Xu, D. Song, J. Li et al., "Electrochemical properties of LiCoO2 + x% S mixture as anode material for alkaline secondary battery," *Electrochimica Acta*, vol. 85, pp. 352–357, 2012.

[5] X. Zeng, J. Li, and B. Shen, "Novel approach to recover cobalt and lithium from spent lithium-ion battery using oxalic acid," *Journal of Hazardous Materials*, vol. 295, pp. 112–118, 2015.

[6] X. Chen, C. Luo, J. Zhang, J. Kong, and T. Zhou, "Sustainable Recovery of Metals from Spent Lithium-Ion Batteries: A Green Process," *ACS Sustainable Chemistry and Engineering*, vol. 3, no. 12, pp. 3104–3113, 2015.

[7] Y. Yao, Y. Cai, G. Wu et al., "Sulfate radicals induced from peroxymonosulfate by cobalt manganese oxides ($Co_xMn_{3-x}O_4$) for Fenton-Like reaction in water," *Journal of Hazardous Materials*, vol. 296, pp. 128–137, 2015.

[8] B. Scrosati and J. Garche, "Lithium batteries: status, prospects and future," *Journal of Power Sources*, vol. 195, no. 9, pp. 2419–2430, 2010.

[9] S. Goriparti, E. Miele, F. De Angelis, E. Di Fabrizio, R. P. Zaccaria, and C. Capiglia, "Review on recent progress of nanostructured anode materials for Li-ion batteries," *Journal of Power Sources*, vol. 257, pp. 421–443, 2014.

[10] R. Ruffo, F. La Mantia, C. Wessells, R. A. Huggins, and Y. Cui, "Electrochemical characterization of LiCoO2 as rechargeable electrode in aqueous LiNO3 electrolyte," *Solid State Ionics*, vol. 192, no. 1, pp. 289–292, 2011.

[11] E. E. Levin, S. Y. Vassiliev, and V. A. Nikitina, "Solvent effect on the kinetics of lithium ion intercalation into $LiCoO_2$," *Electrochimica Acta*, vol. 228, pp. 114–124, 2017.

[12] W. M. Haynes, *CRC Handbook of Chemistry and Physics*, 92nd edition, 2011.

[13] Y. Liu, C. Chang, D. Zhang, and Y. Wu, "Improved electrochemical properties by lithium insertion into Co3O4 in aqueous LiOH solution," *Progress in Natural Science: Materials International*, 2013.

[14] J. Cho, "Correlation of capacity fading of LiMn2O4 cathode material on 55 ∘C cycling with their surface area measured by a methylene blue adsorption," *Solid State Ionics*, vol. 138, no. 3-4, pp. 267–271, 2001.

[15] T. Akar, I. Tosun, Z. Kaynak, E. Kavas, G. Incirkus, and S. T. Akar, "Assessment of the biosorption characteristics of a macrofungus for the decolorization of Acid Red 44 (AR44) dye," *Journal of Hazardous Materials*, vol. 171, no. 1-3, pp. 865–871, 2009.

[16] F. Chai, K. Li, C. Song, and X. Guo, "Synthesis of magnetic porous Fe3O4/C/Cu2O composite as an excellent photo-Fenton catalyst under neutral condition," *Journal of Colloid and Interface Science*, vol. 475, pp. 119–125, 2016.

[17] FullProf Suite, https://www.ill.eu/sites/fullprof/.

[18] http://imagej.nih.gov/ij/download.html.

[19] Y. Baba, S. Okada, and J.-I. Yamaki, "Thermal stability of LixCoO2 cathode for lithium ion battery," *Solid State Ionics*, vol. 148, no. 3-4, pp. 311–316, 2002.